All-optical frequency-resolved optical gating for isolated attosecond pulse reconstruction

Zhen Yang,[1] Wei Cao,[1,]* Xi Chen,[1] Jie Zhang,[1] Yunlong Mo,[1] Huiyao Xu,[1] Kang Mi,[1] Qingbin Zhang,[1] Pengfei Lan,[1] and Peixiang Lu[1,2,3]

[1]*Wuhan National Laboratory for Optoelectronics and School of Physics, Huazhong University of Science and Technology, Wuhan 430074, China*
[2]*Hubei Key Laboratory of Optical Information and Pattern Recognition, Wuhan Institute of Technology, Wuhan 430205, China*
[3]*e-mail: lupeixiang@hust.edu.cn*
*Corresponding author: weicao@hust.edu.cn

We demonstrate an all-optical approach for precise characterization of attosecond extreme ultraviolet pulses. An isolated attosecond pulse is produced from high-order harmonics using an intense driving pulse with a proper gating technique. When a weak field is synchronized with the driver, it perturbs the harmonics generation process via altering the accumulated phase of the electron trajectories. The perturbed harmonic spectrum can be formulated as a convolution of the unperturbed dipole and a phase gate, implying the validity of complete reconstruction of isolated attosecond pulses using a conventional frequency-resolved optical gating method. This *in situ* measurement avoids the central momentum approximation assumed in the widely used attosecond streaking measurement, providing a simple and reliable metrology for an isolated attosecond pulse. © 2020 Optical Society of America

https://doi.org/10.1364/OL.381188

Utilizing the process of high-harmonic generation (HHG) for producing single attosecond (10^{-18} as) pulses [1–3] opens the gate for observing ultrafast dynamics in atoms, molecules, and solids [4–11]. Naturally, it is essential to acquire the complete information of the advanced metrological tool before application. However, for such ultrashort pulses, it is still challenging to directly measure their temporal structure, as there is no means with sufficient temporal resolution for attosecond pulse sampling or available nonlinear materials for an autocorrelation measurement. Fortunately, the short temporal scale of the pulse always implies broad frequency distribution based on the Fourier transform properties, which brings great convenience to characterize attosecond pulses in the frequency domain.

In the past two decades, several schemes have been developed for attosecond pulse characterization in the frequency domain. They are generally divided into two categories: *ex situ* and *in situ* measurements [12]. For the former, the generation and diagnosis of attosecond pulses are performed in different locations while, for the latter, both the generation and measurement are carried out in the same target cell. An *ex situ* scheme such as reconstruction of attosecond beating by interference of two-photon transitions [13], attosecond streak camera [14], and single-color two-photon above-threshold ionization [15], converts extreme ultraviolet (EUV) pulse information into photoelectron momentum and requires precise measurement of the photoelectron spectrum using sophisticated charged particle detecting systems. Today, the most used method for complete characterization of the attosecond pulse is the frequency-resolved optical gating-frequency-resolved optical gating for complete reconstruction of attosecond bursts (FROG-CRAB) method [16]. This method is valid as long as the central momentum approximation is applicable [16]. Nevertheless, for attosecond pulses with low photon energy near the ionization threshold of matter or ultrabroad spectral bandwidth, the application is limited due to the breakdown of the central momentum approximation. As for the *in situ* scheme, it has previously been demonstrated by means of introducing an external second-harmonic pulse for breaking the symmetry, and the emission time of HHG is encoded in the even-order harmonics [17]. Later, Kim *et al.* demonstrated an all-optical scenario for characterizing attosecond pulses in the space-time domain [18]. In that scheme, a weak perturbing pulse propagates non-collinearly with the fundamental with a small deflection angle, and a FROG-like measurement is performed in the space-momentum domain, allowing one to measure the accurate spatial phase of the EUV pulse in the far field. The relative spectral phase in this scheme is acquired via the delay-dependent oscillation at different photon energies. Both *in situ* methods only measure the group delay in HHG, and more complex phase information such as high-order dispersion in an attosecond pulse calls for a more accurate phase retrieval method.

In this Letter, we demonstrate an all-optical approach for accurate characterization of the temporal structure of isolated attosecond pulses. Our approach is inspired by the conventional FROG [19], which has been wildly applied to femtosecond pulse characterization. The conventional FROG trace can be written in the following form:

$$S_0(\omega, \tau) = \left| \int_{-\infty}^{+\infty} E(t) G(t, \tau) e^{i\omega t} dt \right|^2$$

$$= \left| \tilde{E}(\omega) \otimes \tilde{G}(\omega, \tau) \right|^2, \qquad (1)$$

where τ represents the relative delay between the unknown field $E(t)$ and the gate $G(t, \tau)$. The trace also can be expressed in the frequency domain, as shown in the second row of Eq. (1), where $\otimes$ is the convolution operator. $\tilde{E}(\omega)$ and $\tilde{G}(\omega, \tau)$ are the Fourier transform of $E(t)$ and $G(t, \tau)$, respectively. Consequently, waveforms of both $E(t)$ and $G(t, \tau)$ can be extracted via the efficient principal components generalized projection algorithm [20]. A similar reconstruction procedure is also applied in attosecond pulse characterization [15,16], where the photoelectrons are liberated by EUV pulses to form the FROG trace.

In our current all-optical scheme, a strong fundamental field is used to drive high-harmonic radiation [21], and an isolated attosecond pulse can be generated if an optical gating is properly created [22–29]. An additional low-intensity ($< 10^{-2}$) field collinearly propagates with the driving field and perturbs the dynamics of free electrons, which alters the accumulated phase of free electron acquired in the driving field. By scanning the relative delay between the perturbing and driving fields, the spectrum of the attosecond pulse shows strong modulation in both amplitude and central photon energy with respect to delay [see Fig. 1(a)].

When the perturbing field is sufficiently weak, it does not affect the ionization process, but mainly perturbs the free electron's trajectory; then the time-dependent dipole moment can be approximately written as [17]

(a)

(b) (c)

Fig. 1. Principle of the all-optical FROG measurement of an isolated attosecond pulse. (a) When a weak pulse E_s is introduced to perturb the high-harmonic generation process (trace B) driven by the strong pulse E_0, both the amplitude and frequency of the radiated attosecond pulse will be altered depending on the relative delay. (b) Calculated two-dimensional HHG spectrum. (c) Reconstructed (solid lines) and original (dashed lines) attosecond pulses show good agreement in both the intensity profile and temporal phase.

$$d(t, \tau) = \sum_j d_0^j(t) e^{-i\sigma^j(t,\tau)} + \text{c.c.} \qquad (2)$$

$d_0^j(t)$ stands for the dipole moment with only driving field, and the sub-script j stands for the corresponding quantum trajectory. $\sigma^j(t, \tau) = -\int_{t'}^{t(t')} [P_S - A_0(t'')] A_S(t'', \tau) dt''$ is the additional phase induced by the perturbing pulse with t and t' representing the ionization and recombination time, respectively. P_S, A_0 and A_S correspond to the canonical momentum, the vector potential of the driving field, and the perturbing field. If a single attosecond pulse is generated, i.e., a single quantum trajectory is considered, Equation (2) is reduced to $d(t, \tau) = d_0^1(t) e^{-i\sigma^1(t,\tau)} + \text{c.c.}$. The two-dimensional spectrogram trace is obtained by performing the Fourier transform of the dipole acceleration $a(t, \tau) = \ddot{d}(t, \tau)$:

$$S(\omega, \tau) \propto |\tilde{a}(\omega, \tau)|^2 = \omega^4 \left| \tilde{d}(\omega, \tau) \right|^2$$

$$= \omega^4 \left| \tilde{d}_0^1(\omega) \otimes H(\omega, \tau) \right|^2, \qquad (3)$$

where $H(\omega, \tau) = F[e^{-i\sigma^1(t,\tau)}]$ is the Fourier transform of the additional phase induced by the perturbing field. Equation (3) is essentially identical to Eq. (1) with the phase term $e^{-i\sigma^1(t,\tau)}$ serving as a gate in a FROG trace. This implies that both $d_0^1(t)$ and $e^{-i\sigma^1(t,\tau)}$ can be extracted from the spectrogram trace using the standard FROG algorithm.

Figure 1 shows the principle of the all-optical FROG method for attosecond pulse reconstruction. When a few-cycle laser pulse drives HHG, the cut-off harmonic shows a continuous structure, supporting the generation of an isolated attosecond pulse [trace B in Fig. 1(a)]. If a weak field is introduced, the high-harmonic spectrum is perturbed and sensitively depends on the relative delay between the two pulses. We performed the simulation using Lewenstein's model [1], in which the total electric field consisting of the strong driving field and the delayed perturbing field is used for HHG. Here we add a window function on the radiation dipole moment of electron for selecting a single attosecond pulse in a short trajectory region, i.e., mimic the isolate attosecond pulse generation. The calculated two-dimensional neon HHG spectrum generated by a 2×10^{14} W/cm^2, 5 fs, 750 nm driving pulse and a 2×10^{11} W/cm^2, 5 fs, 750 nm perturbing pulse is shown in Fig. 1(b). Comparing the trace in Fig. 1(b) with a typical FROG-CRAB trace, the major difference between them is that the FROG-CRAB trace shows a clear delay-dependent central momentum shift, while the strong yield modulation is a more prominent effect in the trace of the current method. Assuming the spectrogram in Fig. 1(b) can be expressed by Eq. (3), we can then retrieve the attosecond pulse using the PCGP algorithm. The retrieved results are shown in Fig. 1(c), which shows that both the intensity profile and phase of the retrieved attosecond pulse show good agreement with those of the original one, proving the validity of our method.

Our experimental setup is based on a Mach–Zehnder interferometer, as shown in Fig. 2(a). A few-cycle near-infrared pulse centered at 750 nm is split by a 20% reflection beam splitter. The transmission beam serves as a driving field, which passes through the double optical gating (DOG) optics [28,29] for single attosecond pulse generation. A delay stage and an iris are inserted in the reflection beam path for adjusting the relative
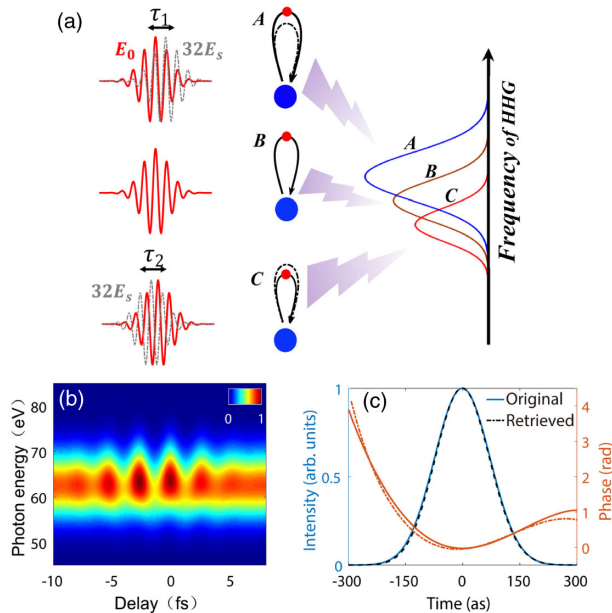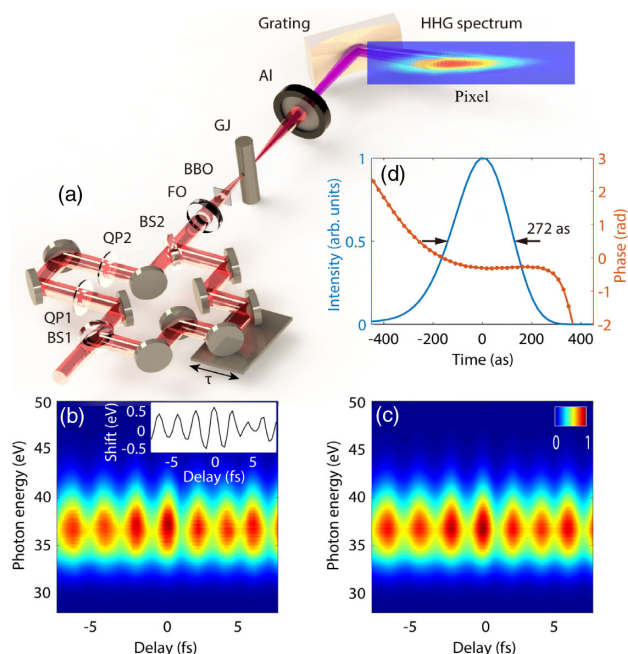
Fig. 2. (a) Experimental layout of the all-optical FROG for isolated attosecond pulse reconstruction. BS, beam splitter; QP1, 330 um quartz plate; QP2, 470 um quartz plate; FO, focusing optics; BBO, barium borate crystal; GJ, gas jet; Al, aluminum film. (b) Measured spectrogram with a delay step size of 400 as. The inset shows the oscillating central photon energy. (c) Retrieved trace. (d) Retrieved temporal profile (blue solid line) and its phase (orange dotted line) of the attosecond pulse.

delay between two pulses and the intensity of the perturbing field, respectively. After that, two beams are recombined by another 20% reflection beam splitter and focused into an argon gas cell for HHG. In the gas cell, the effective intensity in the DOG gate is estimated to be 2×10^{14} W/cm^2, while the leak intensity of the perturbing field is less than 1%. The residual femtosecond near-infrared pulses after the HHG cell are blocked by a 200 nm thick aluminum film. Finally, the spectrum of the attosecond pulse is detected by an EUV spectrometer.

When the DOG optics are properly tuned, supercontinuum harmonic radiation is generated when only the intense driving laser beam is present, as shown in the inset in Fig. 2(a). An attosecond streaking experiment indicates that a single

attosecond pulse has been successfully generated (see Fig. 3). As a delayed weak perturbing field is introduced, both the central photon energy and amplitude of the HHG spectrum are oscillating prominently as a function of delay, as shown in Fig. 2(b). Figure 2(b) resembles the main features of a perturbed harmonic spectrogram as predicted by the simulation in Fig. 1(b). Following the procedure introduced before, we can reconstruct the temporal structure of the dipole moment, i.e., the attosecond pulse. Figure 2(d) shows the retrieved temporal structure of a single attosecond pulse with full width at half-maximum of 272 as.

We also perform an attosecond streaking measurement to compare with our all-optical FROG method. The experimental setup is similar to that in Ref. [30]. The single attosecond pulse and a delayed streaking field are focused into an effusive jet backed with neon gas, and a field-free time of flight spectrometer is used to measure the photoelectron spectrum. Figures 3(a) and 3(b) show the measured and reconstructed streaking traces, respectively. The temporal domain information of the retrieved isolated attosecond pulse is shown in Fig. 3(c). The intensity profile and phase of the retrieved attosecond pulse from the two methods give rather similar results. It should be noted that the central momentum approximation used in the FROG-CRAB measurement may bring errors in retrieving attosecond pulses. In contrast, the all-optical FROG method does not require this approximation and, therefore, is an accurate technique without any critical defect in the reconstruction process, except requiring that the perturbing field is weak enough.

In general, any gating technique should be applicable for the current all-optical method. In Fig. 1, we choose the amplitude gating technique for convenience to illustrate the principle of our method. To verify the validity of our experimental results, we also performed the numerical simulation using DOG with parameters similar to that in the experiment. The time-dependent ellipticity of the driver is formed by two counter-rotating 5 fs, 750 nm few-cycle pulses, and the linear polarized gate for isolated pulse generation has an intensity of 2.35×10^{14} W/cm^2. The perturbing pulse has an intensity of 5×10^{11} W/cm^2. The simulated trace is shown in Fig. 4(a). It exhibits a rather similar trace to the experimental one in Fig. 2(b). Figure 4(c) shows the retrieved attosecond pulse, which is consistent with the original one, confirming that the current method is applicable for the DOG technique. Equation (3) indicates that our scheme is applicable if a single trajectory is selected. To test the generality of our method, we
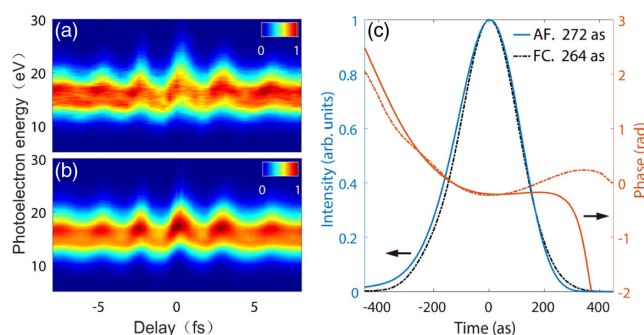

Fig. 3. FROG-CRAB measurement of the isolated attosecond pulse. (a) Measured FROG-CRAB trace of neon gas. (b) Retrieved FROG-CRAB trace. (c) Temporal information of the attosecond pulse retrieved via the all-optical FROG measurement (solid lines) and the FROG-CRAB measurement (dashed lines). In both measurements, the attosecond pulse is generated under the same experimental conditions as Fig. 2.
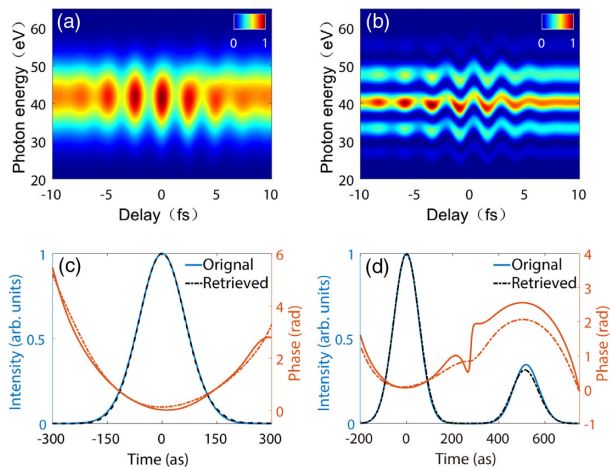
Fig. 4. Numerical analysis of the all-optical FROG measurement of attosecond pulses generated from argon using DOG. (a) Calculated two-dimensional harmonic spectrum when a single trajectory is selected with a window function. (c) Retrieved (solid lines) isolated attosecond pulse from the trace (a) as compared with the original (dashed lines) one. (b) Calculated two-dimensional harmonic spectrum when both short and long trajectories are selected. (d) Retrieved (solid lines) attosecond double pulse from trace (b) as compared with the original one (dashed lines).

consider the case where both short and long trajectories exist. (This can be realized by adding two window functions in the radiation dipole.) The simulated perturbed high-harmonic spectrum is shown in Fig. 4(b). The interference between the two trajectories leads to modulation along the energy axis. Since more than one trajectory is included, strictly speaking, Eq. (3) does not hold, and the retrieved time profile of the attosecond pulses deviates from that of the original one slightly [see Fig. 4(d)]. Nevertheless, the phase information of the two pulses has been properly recovered, and the dual pulse structure is revealed qualitatively, which is indeed valuable information for attosecond experiments.

In conclusion, an all-optical FROG-like measurement has been successfully demonstrated for complete reconstruction of an isolated attosecond pulse. It utilizes a weak field to perturb a single HHG trajectory and forms a FROG trace in the EUV domain. The current approach does not assume the central momentum approximation generally used in the FROG-CRAB measurement and, thus, can be potentially used to diagnose attosecond pulses with more flexible spectral range. It is a convenient and reliable all-optical technique for isolated attosecond pulse characterization with broad application prospects.

Disclosures. The authors declare no conflicts of interest.

REFERENCES

1. M. Lewenstein, P. Balcou, M. Y. Ivanov, A. L'Huillier, and P. B. Corkum, Phys. Rev. A **49**, 2117 (1994).
2. F. Krausz and M. Y. Ivanov, Rev. Mod. Phys. **81**, 163 (2009).
3. P. Lan, P. Lu, W. Cao, Y. Li, and X. Wang, Phys. Rev. A **76**, 011402 (2007).
4. M. Hentschel, R. Kienberger, C. Spielmann, G. A. Reider, N. Milosevic, T. Brabec, P. Corkum, U. Heinzmann, M. Drescher, and F. Krausz, Nature **414**, 509 (2001).
5. R. Kienberger, E. Goulielmakis, M. Uiberacker, A. Baltuska, V. Yakovlev, F. Bammer, A. Scrinzi, T. Westerwalbesloh, U. Kleineberg, U. Heinzmann, and M. Drescher, Nature **427**, 817 (2004).
6. E. Goulielmakis, Z. Loh, A. Wirth, R. Santra, N. Rohringer, V. S. Yakovlev, S. Zherebtsov, T. Pfeifer, A. M. Azzeer, M. F. Kling, S. R. Leone, and F. Krausz, Nature **466**, 739 (2010).
7. H. J. Wörner, J. B. Bertrand, D. V. Kartashov, P. B. Corkum, and D. M. Villeneuve, Nature **466**, 604 (2010).
8. G. Sansone, F. Kelkensberg, J. F. Pérez-Torres, F. Morales, M. F. Kling, W. Siu, O. Ghafur, P. Johnsson, M. Swoboda, E. Benedetti, and F. Ferrari, Nature **465**, 763 (2010).
9. M. Schultze, K. Ramasesha, C. D. Pemmaraju, S. A. Sato, D. Whitmore, A. Gandman, J. S. Prell, L. J. Borja, D. Prendergast, K. Yabana, and D. M. Neumark, Science **346**, 1348 (2014).
10. M. Garg, M. Zhan, T. T. Luu, H. Lakhotia, T. Klostermann, A. Guggenmos, and E. Goulielmakis, Nature **538**, 359 (2016).
11. Z. Tao, C. Chen, T. Szilvási, M. Keller, M. Mavrikakis, H. Kapteyn, and M. Murnane, Science **353**, 62 (2016).
12. K. T. Kim, D. M. Villeneuve, and P. B. Corkum, Nat. Photonics **8**, 187 (2014).
13. P. M. Paul, E. S. Toma, P. Breger, G. Mullot, F. Augé, P. Balcou, H. G. Muller, and P. Agostini, Science **292**, 1689 (2001).
14. J. Itatani, F. Quéré, G. L. Yudin, M. Y. Ivanov, F. Krausz, and P. B. Corkum, Phys. Rev. Lett. **88**, 173903 (2002).
15. A. Kosuge, T. Sekikawa, X. Zhou, T. Kanai, S. Adachi, and S. Watanabe, Phys. Rev. Lett. **97**, 263901 (2006).
16. Y. Mairesse and F. Quéré, Phys. Rev. A **71**, 011401(R) (2005).
17. N. Dudovich, O. Smirnova, J. Levesque, Y. Mairesse, M. Y. Ivanov, D. M. Villeneuve, and P. B. Corkum, Nat. Phys. **2**, 781 (2006).
18. K. T. Kim, C. Zhang, A. D. Shiner, S. E. Kirkwood, E. Frumker, G. Gariepy, A. Naumov, D. M. Villeneuve, and P. B. Corkum, Nat. Phys. **9**, 159 (2013).
19. D. J. Kane and R. Trebino, IEEE J. Quantum Electron. **29**, 571 (1993).
20. D. Kane, IEEE J. Quantum Electron. **35**, 421 (1999).
21. P. B. Corkum, Phys. Rev. Lett. **71**, 1994 (1993).
22. C. Michael, K. Zhao, and Z. Chang, Nat. Photonics **8**, 178 (2014).
23. E. Goulielmakis, M. Schultze, M. Hofstetter, V. S. Yakovlev, J. Gagnon, M. Uiberacker, A. L. Aquila, E. M. Gullikson, D. T. Attwood, R. Kienberger, F. Krausz, and U. Kleineberg, Science **320**, 1614 (2008).
24. P. B. Corkum, N. H. Burnett, and M. Y. Ivanov, Opt. Lett. **19**, 1870 (1994).
25. I. P. Christov, M. M. Murnane, and H. Kapteyn, Phys. Rev. Lett. **78**, 1251 (1997).
26. P. Lan, P. Lu, W. Cao, Y. Li, and X. Wang, Phys. Rev. A **76**, 051801 (2007).
27. W. Cao, P. Lu, P. Lan, X. Wang, and G. Yang, Phys. Rev. A **74**, 063821 (2006).
28. Z. Chang, Phys. Rev. A **76**, 051403(R) (2007).
29. Q. Zhang, P. Lu, P. Lan, W. Hong, and Z. Yang, Opt. Express **16**, 9795 (2008).
30. X. Feng, S. Gilbertson, H. Mashiko, H. Wang, S. D. Khan, M. Chini, Y. Wu, K. Zhao, and Z. Chang, Phys. Rev. Lett. **103**, 183901 (2009).